Study on the enhancement of flow control authority using DBD plasma actuators

Report Number: R24EACA26
Subject Category: JSS Inter-University Research
URL: https://www.jss.jaxa.jp/en/ar/e2024/27502/

Responsible Representative

Tomoaki Tatsukawa, Professor, Tokyo University of Science

Contact Information

Tomoaki Tatsukawa(tatsukawa@rs.tus.ac.jp)

Members

Takuto Ogawa, Tomoaki Tatsukawa, Keita Takigawa, Kevin Tan

Abstract

The objective in this project is to establish active flow control technology using dielectric barrier discharge (DBD) plasma actuators, which are expected to be used in aircraft and other applications. In addition to flow control around an airfoil, this year we will conduct high-fedelity simulations of flow control in more complex flow field involving massive separation phenomena. These simuations aim to expand the applicable range of flow control devices and enhance the effectiveness of active flow control technologies.

Reasons and benefits of using JAXA Supercomputer System

To conduct large-scale three-dimensional unsteady flow simulations using LANS3D, a compressible flow solver with extensive use within our group on JAXA's supercomputer.

Achievements of the Year

In this study, we have been investigating flow separation control methods on an airfoil using a plasma actuator (PA). For the flow around a NACA0015 airfoil at a Reynolds number of 63,000, based on high-fidelity flow field simulations, we previously suggested that control at a non-dimensional frequency of 18, which is higher than the burst frequency typically considered effective at high angles of attack, may be effective.

This year, we focus on controlling the flow around the Ahmed body, which exhibits more complex separation phenomena than the flow around an airfoil. The Ahmed body consists of a rounded front, a long midsection, a slanted rear surface, and a vertical base. Although simplified in geometry, the flow behind the body forms complex three-dimensional structures similar to those seen in aircraft and flying vehicles. This study aims to obtain valuable insights toward practical PA applications by addressing the control of these complex wake flows. Specifically, the slant angle was set to 25 degree, and flow control using PA targeted the separation and longitudinal vortices that form downstream of the model.

To control the flow over the slant surface, we considered multiple PA configurations as shown in Figure 1. These

include: PA1_Counter, installed at the rear edge of the roof inducing flow opposite to the main flow; PA2, installed at the leading edge of the slant inducing flow in the main flow direction; and PA2_Counter, installed at the same location but inducing flow opposite to the main direction. For each configuration, we also tested a case with increased actuator strength, denoted by the suffix _Strong. The baseline case without PA is referred to as Base. The computational grid consisted of approximately 580 million points, and the Reynolds number based on the model height was 200,000. The governing equations were the three-dimensional compressible Navier-Stokes equations. A sixth-order compact finite difference method (alpha = 0.48) was used for spatial discretization, and an ADI-SGS implicit scheme with five inner iterations was used for time integration. The time step was set to dt = 5.0x10^-4. An implicit LES approach was adopted for turbulence modeling. The inflow Mach number was 0.2, with the specific heat ratio gamma = 1.4 and Prandtl number Pr = 0.72.

Figure 2 shows the flow field for the Base. The isosurface represents the second invariant of the velocity gradient tensor, colored by the magnitude of the velocity. A large separation region is formed in the center of the slant, and longitudinal vortices can be observed originating from both sides of the slant. These structures are known from experiments to be characteristic of the Ahmed model with a 25 degree slant angle, and the simulation successfully captures this behavior. Figure 3 shows the velocity distribution in the central cross-section of the slant. The PA2_Strong most effectively suppresses separation on the slant, followed by PA1_Counter_Strong and PA2, in that order. On the other hand, in the PA2_Counter and PA2_Counter_Strong, the separation region actually expands. These results indicate that inducing flow in the main direction is not always effective for controlling separation on the slant. Notably, in the PA1_Counter_Strong, flow reattaches after initially separating at the rear of the roof, and forms along the slant surface, thereby reducing the overall separation region.

Figure 4 shows the distribution of vorticity magnitude near the longitudinal vortices originating from the slant edges. In the PA2_Counter_Strong, vortices decay toward the rear edge of the slant, whereas in the PA1_Counter_Strong, which showed strong separation suppression, little influence on the longitudinal vortices is observed. This difference likely stems from the spatial relationship between the slant separation shear layer and the longitudinal vortices. A more detailed investigation of the flow structures near the model edges could reveal a way to indirectly control longitudinal vortices by properly manipulating the shear layer.

In summary, the results demonstrate that it is possible to suppress flow separation over the slant of the Ahmed body using PA. Furthermore, weakening of longitudinal vortices can also be achieved through separation control. The effectiveness of this influence varies significantly depending on the control conditions. We will focus on clarifying the relationship between the flow near the model's edges and the separation shear layer over the slant, in order to identify improved methods for longitudinal vortex control.

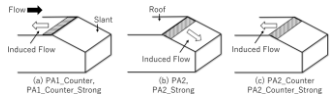

Fig. 1: PA installation condition

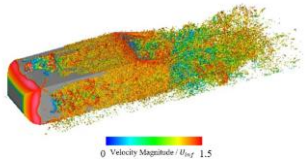

Fig. 2: Instantaneous flow-field of Base case (Iso-suraface is the 2nd invariant of the velocity gradient tensors)

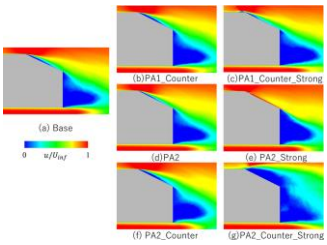

Fig. 3: Streamwise velocity distribution at the central cross-section of the model

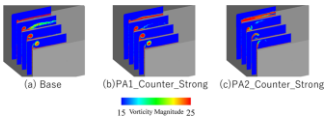

Fig. 4: Distribution of vorticity magnitude around the streamwise vortices

Publications

- Oral Presentations

K. Takigawa, K. Asada, K. Watanabe, T. Tatsukawa, K. Fujii, "LES of Flows Controlled by a DBD Plasma Actuator on a Slant of. the Ahmed Model", CFD38, Tokyo, Dec. 2024.

- Poster Presentations

K. Takigawa, K. Asada, K. Watanabe, T. Tatsukawa, K. Fujii,“Flow Control over a Slant of the Ahmed Model Using a DBD Plasma Actuator”,The 11th Symposium of the Plasma Actuator Research Committee, Fluid Engineering Division, The Japan Society of Mechanical Engineers (JSME), Online, Jan. 2025.

Usage of JSS

Computational Information

Process Parallelization Methods	MPI
Thread Parallelization Methods	Automatic Parallelization
Number of Processes	79 - 269
Elapsed Time per Case	24 Hour(s)

- **JSS3 Resources Used**

Fraction of Usage in Total Resources[*1](%): 0.46

Details

Computational Resources		
System Name	CPU Resources Used (core x hours)	Fraction of Usage[*2](%)
TOKI-SORA	12,498,425.60	0.57
TOKI-ST	0.00	0.00
TOKI-GP	0.00	0.00
TOKI-XM	0.00	0.00
TOKI-LM	0.00	0.00
TOKI-TST	0.00	0.00
TOKI-TGP	0.00	0.00
TOKI-TLM	0.00	0.00

File System Resources		
File System Name	Storage Assigned (GiB)	Fraction of Usage[*2] (%)
/home	40.00	0.03
/data and /data2	35,400.00	0.17
/ssd	0.00	0.00

Archiver Resources		
Archiver Name	Storage Used (TiB)	Fraction of Usage[*2] (%)
J-SPACE	0.00	0.00

[*1]: Fraction of Usage in Total Resources: Weighted average of three resource types (Computing, File System, and Archiver).

[*2]: Fraction of Usage：Percentage of usage relative to each resource used in one year.

- **ISV Software Licenses Used**

ISV Software Licenses Resources		
	ISV Software Licenses Used (Hours)	Fraction of Usage[*2] (%)
ISV Software Licenses (Total)	0.00	0.00

[*2]: Fraction of Usage：Percentage of usage relative to each resource used in one year.